A Calmodulin-Regulated Protein Kinase Linked to Neuron Survival Is a Substrate for the Calmodulin-Regulated Death-Associated Protein Kinase†

Andrew M. Schumacher, James P. Schavocky, Anastasia V. Velentza,‡ Salida Mirzoeva,§ and D. Martin Watterson*

Drug Discovery Program, Northwestern University Feinberg School of Medicine, Chicago, Illinois 60611

Received February 28, 2004; Revised Manuscript Received April 22, 2004

ABSTRACT: Death-associated protein kinase (DAPK) is a calmodulin (CaM)-regulated protein kinase and a drug-discovery target for neurodegenerative diseases. However, a protein substrate relevant to neuronal death had not been described. We identified human brain CaM-regulated protein kinase kinase (CaMKK), an enzyme key to neuronal survival, as the first relevant substrate protein by using a focused proteomics- and informatics-based approach that can be generalized to protein kinase open reading frames identified in genome projects without prior knowledge of biochemical context. First, DAPK-interacting proteins were detected in yeast two-hybrid screens and in immunoprecipitates of brain extracts. Second, potential phosphorylation site sequences in yeast two-hybrid hits were identified on the basis of our previous results from positional-scanning synthetic-peptide substrate libraries and molecular modeling. Third, reconstitution assays using purified components demonstrated that DAPK phosphorylates CaMKK with a stoichiometry of nearly 1 mol of phosphate per mole of CaMKK and a K_m value of 3 μM. Fourth, S511 was identified as the phosphorylation site by peptide mapping using mass spectrometry, site-directed mutagenesis, and Western blot analysis with a site-directed antisera targeting the phosphorylated sequence. Fifth, a potential mechanism of action was identified on the basis of the location of S511 near the CaM recognition domain of CaMKK and demonstrated by attenuation of CaM-stimulated CaMKK autophosphorylation after DAPK phosphorylation. The results raise the possibility of a CaM-regulated protein kinase cascade as a key mechanism in acute neurodegeneration amenable to therapeutic targeting.

Death-associated protein kinase (DAPK)[1] is a calmodulin (CaM)-regulated serine/threonine protein kinase that is a drug-discovery target for neurodegenerative disease (*1*). For example, in vivo treatment with a bioavailable small-molecule inhibitor of DAPK in a pharmacologically relevant time window of hours after injury enhances neuronal survival and reduces brain tissue loss in an animal model of stroke (*2*). However, the downstream events in the DAPK-mediated signal transduction pathways involved in acute neurodegeneration after brain injury and rescue by DAPK-targeted experimental therapeutics are not known. This knowledge is key for understanding the role of DAPK-mediated death pathways in neurodegenerative disorders and gaining insight into response to therapeutic intervention.

The identification of biologically relevant protein substrates from brain is a minimal, but critical, next step because the profile of protein substrates for a particular kinase determines the functional role for that protein kinase. For example, cyclic AMP-dependent protein kinase (PKA), one of the first protein kinases characterized in detail (*3*), has diverse protein substrates but has discrete biological functions that reflect the available protein substrates and convergence with other signal transduction pathways (*4*). DAPK, in contrast to PKA and many other serine/threonine protein kinase family members, appears to have fairly strict substrate requirements based on quantitative activity analyses with positional-scanning peptide-substrate libraries (*5*) and the failure of many standard protein and peptide substrates to serve as effective substrates for DAPK. This makes identification of DAPK substrates a challenge. In addition, the post-genome sequence era has identified additional barriers in that there is not a generally accepted approach for the elucidation of protein kinase-mediated pathways that start with the identification of the kinase as an open reading frame (ORF). This requires that investigations start with a protein kinase ORF in the absence of a biochemical context and move downstream in the signal transduction pathway to identify substrates versus the established historical precedent of starting with substrate-mediated downstream events followed by identification of the upstream kinase(s) (*3*, *6*).

One approach for the elucidation of DAPK-mediated signal transduction pathways is to utilize structure-assisted, enzymology-based approaches as a starting point, thereby providing a foundation and focus to experimental design and data interpretation. This approach was applied to the initial investigations (*5*), for example, that established a robust,

† This work was supported in part by grants from the National Institutes of Health (Grants NS047586, AG00260, and RR13810).

* Corresponding author: Mailing address: Northwestern University Medical School, Ward 8-196, 303 E. Chicago Ave., Chicago, IL 60611. Tel: (312)503-0656. E-mail: m-watterson@northwestern.edu.

‡ Current address: Genomics Institute of Novartis Research Foundation, San Diego, CA.

§ Current address: Department of Medicine, Northwestern University, Chicago, IL.

[1] Abbreviations: CaM, calmodulin; CaMKK, calmodulin-dependent protein kinase kinase; CaMKIV, calmodulin-dependent protein kinase IV; PKA, cyclic AMP-dependent protein kinase; DAPK, death-associated protein kinase; IP, immunoprecipitation; MALDI-TOF MS, matrix-assisted laser desorption time-of-flight mass spectrometry; MAPK, mitogen-activated protein kinase; MLC, myosin light chain; MLCK, myosin light chain kinase; ORF, open reading frame.

10.1021/bi049589v CCC: $27.50
Published on Web 06/04/2004

quantitative activity assay for in vivo experiments (*7*) and inhibitor discovery (*2*). As a logical extension of this approach, we initiated a search for potential endogenous protein substrates for DAPK relevant to neuronal death. The combined use of yeast two-hybrid screens, immunoprecipitation of brain tissue lysates, and phosphotransferase experiments identified CaMKK as a potentially relevant substrate. Analysis of kinetics and stoichiometry of phosphorylation identified CaMKK as a potential endogenous brain substrate based on a K_m value that falls within the 1−20 μM range and stoichiometric phosphate incorporation into a discrete site, characteristic features of physiological substrates for intracellular, signal-transducing protein kinases (*8*). The placement of the phosphorylation site within the CaMKK amino acid sequence suggested a potential mechanism of DAPK-mediated down regulation of the neuronal pathway that requires CaMKK autophosphorylation as an early activating event. The feasibility of this hypothesis was probed by demonstration of an attenuated CaMKK autophosphorylation response. The results provide a firm foundation for future investigations and raise the possibility that a CaM-regulated protein kinase cascade may be critical in injury-induced neuronal apoptosis.

EXPERIMENTAL PROCEDURES

Yeast Two-Hybrid Screening of Human Brain cDNA Library. Yeast two-hybrid screens were done with the Matchmaker system (BD Biosciences Clontech, Palo Alto, CA) using a DAPK bait lacking the CaM-regulation domain (DAPKΔCaM). To create the bait, site-directed mutagenesis (Stratagene, La Jolla, CA) of the DAPK cDNA (accession no. X76104) was done using the primers 5′-CTAAAGATACACAACAGGCACTTAGTTCACTGTGCCAAAGATTATCCAGGTC-3′ and 5′-GACCTGGATAATCTTTGGCACAGTGAACTAAGTGCCTGTTGTGTATCTTTAG-3′, resulting in a DAPKΔCaM cDNA in which amino acid residues 288−312 were deleted. The DAPKΔCaM cDNA was inserted in the pGBKT7 vector as a fusion with the Gal4 DNA-binding domain by PCR subcloning using the primers 5′-CGGAATTCATGACCGTGTTCAGGCAGGAAAACG-3′ and 5′-GCGTCGACTCACCGGGATACAACAGAGC-3′. The human brain cDNA library (BD Biosciences Clontech, Palo Alto, CA) was in the pACT2 vector as a fusion with the Gal4 transcriptional activation domain.

Yeast two-hybrid screens were performed essentially as described by the manufacturer with the yeast strain AH109 transformed simultaneously with each plasmid by heat shock. One hundred positive colonies were replated four times. Plasmid DNA was extracted (Zymo Research, Orange, CA) from 67 restreaked colonies, the cDNA inserts were amplified by PCR using primers (BD Biosciences Clontech, Palo Alto, CA) against the pACT2 vector at the 5′ and 3′ ends of the multiple cloning site, and the PCR products were sequenced.

Analysis of ORFs for the Presence of Potential Phosphorylation Sites. DNA sequences obtained from yeast two-hybrid screening were searched against Genbank using NCBI BLAST (http://www.ncbi.nlm.nih.gov), and the ORFs of hypothetical proteins found in the nucleotide BLAST search were subjected to protein−protein BLAST search. The resulting ORFs were then searched for the presence of potential DAPK phosphorylation motifs as previously described (*5*). Further database search of the Swissprot and trEMBL databases in the *Homo sapiens* taxon and analysis of sequence patterns were done using ScanProsite (http://us.expasy.org/tools/scanprosite) with the pattern [IKR]-[IKR]-X-X-[RS]-[ARTS]-[FILMPSTY]-*[ST]*-[ADKNST]-X-X-X-X-X-X-X-[KRST], where X is any residue, and the italicized *ST* is the phosphorylated residue assigned position P0.

Immunoprecipitation (IP) of Endogenous Brain DAPK and Western Blotting. Mouse-anti-DAPK IgG_1 (Sigma Aldrich, St. Louis, MO), goat-anti-CaMKKβ (Santa Cruz Biotechnology, Santa Cruz, CA), or mouse preimmune IgG_1 (Chemicon International, Temecula, CA) was coupled to AminoLink Plus resin (Pierce Biotechnology, Rockford, IL) using the manufacturer's protocol and resuspended in phosphate-buffered saline. Soluble extracts from whole Sprague−Dawley rat brain (2.5 g) were prepared in a Dounce homogenizer in RIPA buffer (20 mM Tris, pH 7.5, 1 mM EDTA, 150 mM NaCl, 0.5% NP-40, 0.1 mM $NaVO_3$, 1 mg/L leupeptin, 1 mg/L pepstatin, 40 μM *N*-α-*p*-tosyl-L-lysine chloromethyl ketone, TLCK), followed by centrifugation (3 × 15 min, 15 000*g*, 4 °C). The homogenate supernatant (100 μg) was incubated with the AminoLink Plus-coupled antibodies (25 μL resin) for 2 h at 4 °C. Each immunoprecipitation (IP) was centrifuged 4 min at 2000*g*. Pellets were washed once with RIPA buffer and twice with 20 mM Tris, pH 7.5, 1 mM EDTA. Bound protein was eluted by boiling in SDS−PAGE sample buffer (100 mM Tris, pH 7.0, 2% SDS, 10% glycerol, 5 mM dithiothreitol). Proteins were resolved by SDS−PAGE and analyzed by Western blot analysis essentially as previously described (*9*) using polyclonal antibodies against DAPK and CaMKKβ (Santa Cruz Biotechnology, Santa Cruz, CA).

Incorporation of phosphate into IP mixtures was done by resuspension and incubation for 10 min at 25 °C in assay buffer (20 mM Hepes, pH 7.5, 1 mM DTT, 2 mM $MgCl_2$, 2 mM $MnCl_2$, 75 mM NaCl) containing 200 μM ATP and [γ^{32}P]-ATP (2.5 μCi per reaction). Reactions in the presence of small molecule inhibitors were done by addition of either 20 μM DAPK inhibitor (*2*) or 75 μM K252c, a more general protein kinase inhibitor (*10*) that inhibits CaMKK but not DAPK (Schumacher and Watterson, unpublished data). Reactions were terminated by adding SDS−PAGE sample buffer, products were resolved by SDS−PAGE, and phosphorylated proteins were visualized by phosphor-image analysis (STORM, Amersham Biosciences, San Francisco, CA).

Protein Production. The human CaMKKβ cDNA (accession no. AF140507, Stratagene, La Jolla, CA) was subcloned into the pGEX-4T-1 vector (Amersham Biosciences, San Francisco, CA) using the primers 5′-CGCGCGGGATCCATGTCATCATGTGTCTCTAGCC-3′ and 5′-CCGCTCGAGTCACTCGGGCTCCATGGCCTCCTCC-3′, creating an amino-terminal fusion with the glutathione-S-transferase (GST) cDNA. The K194A substitution was made by site-directed mutagenesis (Stratagene, La Jolla, CA) using the primers 5′-CAATACCTACTATGCAATGGCGGTGCTGTCCAAAAAGAAGC-3′ and 5′-GCTTCTTTTTGGACAGCACCGCCATTGCATAGTAGGTATTG-3′. The S509A mutation was made using the primers 5′-AGCCGGCGGGAGGAACGCGCACTGTCAGCGCCTGGAAACT-3′ and 5′-AGTTTCCAGGCGCTGACAGTGCGCGTTCCTCCCG-

CCGGCT-3′. The S511A mutation was made using the primers 5′-GGCGGGAGGAACGCTCACTGGCAGCGC-CTGGAAACTTGCT-3′ and 5′-AGCAAGTTTCCAGGCG-CTGCCAGTGAGCGTTCCTCCCGCC-3′. The T518A mutation was made using the primers 5′-GCGCCTGGAAACT-TGCTCGCCAAAAAACCAACCAGGGAAT-3′ and 5′-ATTCCCTGGTTGGTTTTTTGGCGAGCAAGTTTCCAG-GCGC-3′. Plasmids were transformed into BL21 *Escherichia coli*.

For protein expression, 4 L cultures were grown in Luria Broth (Invitrogen, Carlsbad, CA) at 37 °C to an optical density of 0.75 at 600 nm and induced with 0.1 mM isopropyl β-D-thiogalactopyranoside. Cultures were grown for 2 h, and bacteria were harvested by centrifugation at 5000*g*. Cell pellets were lysed by sonication in lysis buffer (20 mM, Tris, pH 7.5, 1 mM EDTA, 1 mM DTT, 150 mM NaCl, 1 mg/L leupeptin, 1 mg/L pepstatin, 40 μM TLCK, 0.02% Triton X-100). The homogenate was clarified by centrifugation at 10 000*g* for 15 min, and the supernatant was applied to a 10 mL glutathione−agarose column (Sigma Aldrich, St. Louis, MO) equilibrated with column buffer (20 mM Tris, pH 7.5, 1 mM DTT, 1 mM EDTA, 150 mM NaCl). The column was treated with 10 volumes of column buffer, and GST−CaMKKβ was step-eluted with 5 volumes of column buffer containing 1 mM reduced glutathione. Further purification of GST−CaMKKβ was done by adding $CaCl_2$ to a final concentration of 2 mM and subjecting to CaM affinity-based chromatography (*11*) using 1 mL of commercially available (Amersham Biosciences, San Francisco, CA) CaM−sepharose resin. Proteins were applied using column buffer containing 2 mM $CaCl_2$ but lacking EDTA and desorbed by elution with column buffer containing 2 mM EGTA. Proteins were concentrated by centrifugation at 5000*g* at 4 °C using spin concentrators (Pall Corporation, East Hills, NY) rated for MW 30 000 cutoff and buffer-exchanged to 20 mM Tris, pH 7.5, 1 mM DTT, 1 mM EDTA.

The clone for GST−syntaxin 1A was provided by Dr. Zu-Hang Sheng (National Institutes of Health) in the pGEX-4T-1 vector and was expressed and purified using glutathione−agarose chromatography as described above for GST−CaMKKβ. Constitutively active DAPK catalytic domain protein (*5*) and smooth muscle myosin light chain (MLC) from chicken gizzard (*12*) were made as previously described.

Activity Assays. Activity assays were carried out as follows: The substrate proteins were incubated with 200 μM ATP and [γ^{32}P]-ATP (2.5 μCi per reaction) in assay buffer (20 mM Hepes, pH 7.5, 1 mM DTT, 2 mM $MgCl_2$, 2 mM $MnCl_2$, 75 mM NaCl) for 15 min at 25 °C, either with or without the DAPK catalytic domain protein (0.5 μM). Reactions were initiated by addition of DAPK. For kinetics experiments, reactions were spotted onto P-81 paper (Whatman, Clifton, NJ), washed with 75 mM H_3PO_4 and 95% EtOH, and quantified by scintillation counting in EcoScint O (National Diagnostics, Atlanta, GA). Data were plotted on a double-reciprocal graph and analyzed by linear regression using the Prism software package (version 3.03, Graphpad Software Inc., San Diego, CA). To verify the values estimated by double-reciprocal plotting, K_m values were also determined by nonlinear curve fitting to the Michaelis−Menton equation weighted by $1/V^2$ using Prism. Stoichiometry experiments were performed using 1.35 μM GST−CaMKKβ(K194A) incubated with DAPK for the indicated times. DAPK was added each hour starting at time 0 min. Reactions used for phosphorylation site mapping by Western blotting were done as described for stoichiometry experiments except [γ^{32}P]-ATP was not used. Reactions were terminated by adding SDS−PAGE sample buffer, resolved by SDS−PAGE, and analyzed by Western blotting. Site-directed phospho-CaMKKβ polyclonal antisera (number 6410) was made, using a previously described protocol for antibody production (*13*), against the synthetic peptide REERSL(pS)APGNLC that contained a phosphorylated serine corresponding to S511 of CaMKKβ.

CaMKK autophosphorylation experiments were performed using the reaction buffers and temperatures described above with the following exceptions: GST−CaMKKβ (0.86 μM) was first incubated with or without DAPK (0.5 μM) for 5 min in a reaction lacking [γ^{32}P]-ATP. Then [γ^{32}P]-ATP (2.5 μCi per reaction) was added with or without 1 mM $CaCl_2$ and 1 μM CaM. The reactions were incubated an additional 5 min so that CaMKK autophosphorylation would result in ^{32}P incorporation. Reactions were terminated by adding SDS−PAGE sample buffer, products were resolved by SDS−PAGE, and proteins were stained with Coomassie blue R-250 to verify equal protein loading. Incorporation of ^{32}P was visualized by phosphor-image analysis, and band density was measured using ImageQuant software (Amersham Biosciences, San Francisco, CA).

Identification of Phosphorylation Sites by MALDI-TOF MS. GST−CaMKKβ(K194A) (1.35 μM) or GST−syntaxin 1A (8.5 μM) were phosphorylated with DAPK (0.5 μM) as described for stoichiometry experiments, except that non-radioactive ATP was used. Streptactin−sepharose (Sigma-GenoSys, The Woodlands, TX) was used to remove the epitope-tagged DAPK (*5*). Proteins were precipitated with trichloroacetic acid, the mixture was centrifuged, the pellet was washed with acidified ethanol and resuspended in 0.1 M NH_4HCO_3, and the pH 8 solution was incubated with trypsin−*N*-tosyl-L-phenylalanine chloromethyl ketone (TPCK) (1:20 w/w) for 16 h at 37 °C, and the resulting peptides were separated by HPLC (AB130A, Applied Biosystems, Foster City, CA) on a C8 column with a 0%−60% acetonitrile gradient in 0.1% trifluoroacetic acid (TFA). Masses were analyzed by MALDI-TOF MS (Voyager DE-RP, PE Biosystems, Foster City, CA) using saturated α-cyano-hydroxycinnamic acid matrix in 50% acetonitrile and 0.15% TFA. Theoretical peptide masses were obtained by performing the trypsin digest function of the Protean software package (DNAStar, Madison, WI) on the ORFs of the substrate proteins. One unit was added to the masses to obtain the expected MH^+ value of each peptide.

Transfection of Human Cell Line with Plasmid Encoding Constitutively Active DAPK. The constitutively active DAPK catalytic domain (*5*) was subcloned into the pTracer-CMV2 mammalian expression vector (Invitrogen, Carlsbad, CA) using the primers 5′-GGGGTACCATGGCCGTGTTCAG-GCAGGAAAACGTGG-3′ and 5′-CGGAATTCTCAAC-TAAGTGCCTGTTGTGTATCTTTAG-3′. Human SH-SY5Y neuroblastoma cells were plated in 24-well plates in αMEM (Mediatech, Herndon, VA) containing 10% fetal bovine serum and 1% antibiotics (100 U/mL penicillin and 100 μg/mL streptomycin, Invitrogen, Carlsbad, CA). At 95% con-

fluency, cells were transfected with 1 μg of DAPK plasmid or 1 μg of CMV-EGFP control plasmid (plasmid no. 2145, kindly provided by Dr. Ashok Aiyar, Northwestern University) using Lipofectamine 2000 as described in the manufacturer's instructions (Invitrogen, Carlsbad, CA). Six hours after transfection, cells were washed twice with PBS, and lysates were collected in SDS−PAGE sample buffer. Protein content was determined by the BCA method (Pierce Biotechnology, Rockford, IL), and equal protein was used for Western blot analysis with antibodies against phospho-CaMKKβ(S511) and the DAPK catalytic domain (*5*).

RESULTS

Identification of CaMKK as a DAPK-Interacting Protein with a Potential DAPK Phosphorylation Site Sequence. As an initial screen to detect potential DAPK-interacting proteins, we performed a yeast two-hybrid screen of a human brain cDNA library. A full-length human DAPK bait missing its CaM regulatory domain was used to prevent the high-affinity interactions with abundant CaM encoding clones. The sequences of the cDNA inserts from 67 positive clones from the yeast two-hybrid screen were searched against GenBank. All six possible open reading frames from the GenBank hits were searched for the presence of a DAPK phosphorylation site motif. This identified CaMKKβ as a DAPK-interacting protein containing a potential phosphorylation site amino acid sequence (RREERSLSA). The potential DAPK phosphorylation site in CaMKK is found at a region near the carboxy-terminal side of the CaM recognition domain of CaMKK. The CaMKKα isoform, which has a 65% amino acid sequence similarity to CaMKKβ, has a similar potential phosphorylation site sequence (RREERSMSA). Because of the prior linkage between CaMKK and neuronal survival (*14*), priority was given to further characterization of this potential interaction.

We used coimmunoprecipitation from brain lysates as a secondary screen to demonstrate the relevance of the yeast two-hybrid results to interactions of endogenous proteins in brain. First, we performed an immunoprecipitation using anti-DAPK antibodies and screened for the presence of CaMKK in the immunoprecipitate. Western blot analysis of the immunoprecipitate revealed the presence of CaMKK (Figure 1A, lane 1). Second, we did a reverse immunoprecipitation experiment with antibodies directed against CaMKKβ and showed the presence of DAPK in the immunoprecipitate (Figure 1A, lane 2).

As a tertiary screen testing the potential significance of these endogenous proteins to a kinase−substrate interaction, we incubated the anti-DAPK immunoprecipitate with [γ^{32}P]-ATP in the presence or absence of protein kinase inhibitors and analyzed reaction products by autoradiography after gel electrophoresis. Figure 1B shows that several proteins in the DAPK immunoprecipitate are phosphorylated (Figure 1B, lane 1), including one with an electrophoretic mobility consistent with CaMKKβ, as determined by Western blots run in parallel. There is also a phosphorylated protein with an electrophoretic mobility of approximately 56 000, the apparent chain weight of the CaMKKα isoform, which was also detected by Western blot analysis of the DAPK immunoprecipitate (data not shown). The phosphorylation of these proteins was reduced (Figure 1B, lane 2) when the incubation was done in the presence of a selective DAPK inhibitor but not in the presence of a more general protein kinase inhibitor that does not inhibit DAPK (Figure 1B, lane 3). These results are consistent with the observed phosphorylation being due primarily to DAPK and not due to CaMKK autophosphorylation or other contaminating kinases in the immunoprecipitate. The data confirm and extend the yeast two-hybrid screen results and indicate an enzyme−substrate relationship.

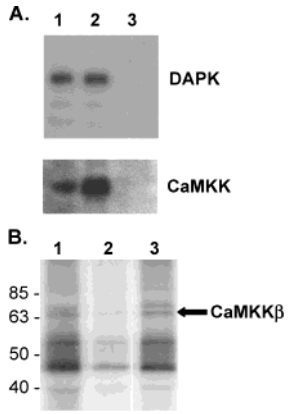

FIGURE 1: Coimmunoprecipitation and phosphorylation of CaMKK by DAPK. In panel A, DAPK and CaMKKβ were immunoprecipitated from rat brain and analyzed by Western blot for DAPK and CaMKKβ: DAPK immunoprecipitate (lane 1); CaMKKβ immunoprecipitate (lane 2); control IgG_1 immunoprecipitate (lane 3). Note that CaMKK coimmunoprecipitated with DAPK and vice versa. In panel B, DAPK immunoprecipitates were incubated with [γ^{32}P]-ATP and analyzed by phosphor-imaging to determine phosphorylation of coimmunoprecipitated proteins (lane 1). To assess specificity, the reactions were incubated with a DAPK inhibitor (*2*) (lane 2) or K252c (lane 3). The arrow indicates a coimmunoprecipitated protein that migrates like CaMKKβ (64 kD) in SDS−PAGE as determined by the R_f value in a parallel Western blot.

CaMKK as a DAPK Substrate. Eukaryotic signal-transducing protein kinases generally have K_m values for physiological protein substrates in the range of 1−20 μM with stoichiometric incorporation of phosphate into a single site or set of sites (*8*). To characterize this aspect of DAPK-mediated phosphorylation of CaMKK, we used purified proteins expressed in *E. coli*, which lacks serine/threonine protein kinases, in reconstitution assays. To remove the contribution of CaMKK autophosphorylation to the total phosphate incorporation during the time course of enzyme incubations, we engineered a catalytically inactive mutant CaMKK, CaMKKβ(K194A), that cannot undergo autophosphorylation. Therefore, any phosphate incorporated into CaMKKβ(K194A) by incubation with ATP and DAPK would quantify only DAPK phosphotransferase activity with CaMKK as a protein substrate. The phosphor-imaging results shown in the Figure 2A insert demonstrate that radioactive phosphate is incorporated into CaMKKβ(K194A) only when DAPK is present. Under these conditions, DAPK catalyzes approximately 1 mol of phosphate incorporation per mole of CaMKK substrate (Figure 2A), consistent with a single site. The site was identified in later studies, summarized in a subsequent section of this report.

Kinetic analysis of the DAPK phosphorylation of CaMKKβ-(K194A) by varying substrate concentration revealed an estimated K_m value of approximately 3 μM (Figure 2B) and a V_{max} of 0.087 pmol of phosphate/min/pmol of DAPK.

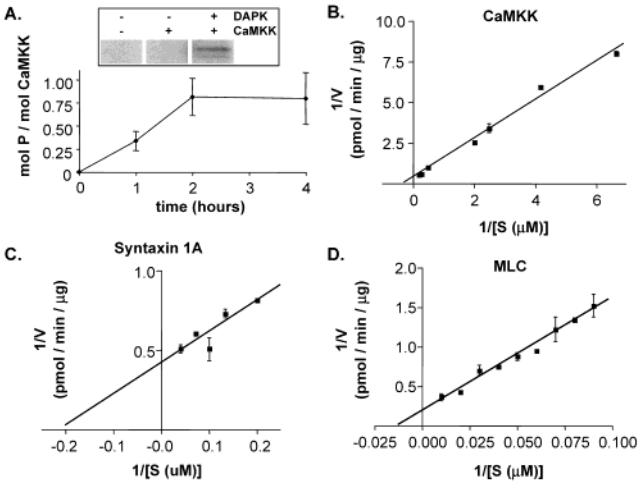

FIGURE 2: Characterization of DAPK-catalyzed protein substrate phosphorylation. The phosphorylation of purified protein substrates was done as described in Experimental Procedures. In all panels, data points and error bars show the mean ± SEM. Error bars are not shown if SEM is smaller than the symbol; r^2 is the goodness of fit in the linear regression analyses. In panel A, stoichiometry of CaMKKβ phosphorylation by DAPK was determined by incubation of DAPK with the substrate GST−CaMKKβ(K194A) for 0−4 h and quantified by scintillation counting of ^{32}P-incorporation into substrate. Data are from two independent experiments. In the inset, phosphorylation of the GST−CaMKKβ band was visualized by phosphor-imaging. Either DAPK alone, catalytically inactive GST−CaMKKβ(K194A) alone, or DAPK and GST−CaMKKβ(K194A) were used for in vitro reactions. In panel B, the K_m value for DAPK phosphorylation of CaMKKβ was determined in reactions where the concentration of the substrate, GST−CaMKKβ(K194A), was varied from 0.15 to 5 μM. Data were analyzed by double-reciprocal plot and linear regression ($r^2 = 0.98$). The *x*-intercept reflects the K_m value. Data are from two independent experiments. In panel C, the K_m value for DAPK phosphorylation of GST−syntaxin 1A was determined as done for CaMKK. Concentration of syntaxin 1A was varied from 5 to 25 μM. Data are from two independent experiments ($r^2 = 0.72$). In panel D, the K_m value for DAPK phosphorylation of myosin light chain (MLC) was determined by varying the concentration of MLC from 11 to 100 μM. Data are representative of two independent experiments ($r^2 = 0.93$).

These values compare well to those that we obtained with another brain substrate for DAPK, syntaxin 1A. Syntaxin 1A, a brain DAPK substrate not linked to neuronal death, was serendipitously discovered (*15*) in yeast two-hybrid screens for potential syntaxin 1A binding partners. We found that it has a K_m value of approximately 5 μM with DAPK (Figure 2C) and also has a V_{max} of 0.087 pmol of phosphate/min/pmol of DAPK. In contrast to the close similarity between these two brain-derived DAPK substrates, DAPK has a K_m of approximately 65 μM (Figure 2D) for smooth muscle myosin light chain (MLC). MLC has been previously reported to be a DAPK substrate (*16*). The finding that syntaxin 1A and CaMKK have very different sequences around the potentially phosphorylatable serine residue yet have similar kinetic properties indicates that divergent phosphorylation site sequences can be accommodated by DAPK in protein substrates. These novel findings warranted further investigation of the DAPK phosphorylation site in CaMKK.

DAPK Phosphorylation Site in CaMKK. In addition to confirming the intriguing finding that DAPK apparently uses divergent phosphorylation site sequences in protein substrates from the same tissue, knowledge of the site of DAPK phosphorylation in CaMKK has the potential to provide insight into how DAPK phosphorylation might regulate CaMKK activity. We used standard proteomics methods to map the proposed site of phosphorylation in CaMKK, then confirmed and extended the results by site-directed mutagenesis and by Western blot analysis using site-directed phosphoprotein antisera. CaMKKβ(K194A) was phosphorylated by DAPK or subjected to identical treatments in the absence of DAPK phosphorylation as a control and then digested with trypsin. The resulting peptide mixtures for CaMKK control and phosphorylated CaMKK were fractionated by reverse-phase liquid chromatography, and effluent fractions were analyzed by MALDI-TOF MS. The experimentally obtained masses were compared to the expected masses computed for each peptide. The goal was to determine whether the apparent mass of the peptide containing the proposed phosphorylation site serine was changed by intervals of approximately 80, indicating the presence of one or more phosphate groups.

Table 1: Identification of DAPK Phosphorylation Sites in CaMKK and Syntaxin 1A by MALDI-TOF MS Analysis[a]

peptide	peptide mass detected (expected) −DAPK	+DAPK
	CaMKKβ	
1. SL**S**APGNLLTK	1100.18 (1100.26)	**1180.10** (**1180.26**)
2. SFGNPFEGSR	1096.34 (1097.14)	1096.60 (1177.14)
3. GSSSSESQKPCEALR	1564.68 (1565.66)	1566.05 (1645.66)
4. GSMSSCVSSQPSSNR	1513.87 (1513.61)	1514.48 (1593.61)
	Syntaxin 1A	
5. TTTSEEL...IIMDSSI**S**K	3275.22 (3273.61)	**3351.02** (**3353.61**)
6. ELHDMF...ESQEMIDR	2628.36 (2629.07)	2629.91 (2709.07)
7. HSAILASPNPDEK	1380.41 (1378.49)	1379.01 (1458.49)

[a] Purified CaMKK and syntaxin 1A were treated with purified DAPK and ATP (+DAPK) or with ATP alone (−DAPK), protein mixtures were digested with trypsin, digestion mixtures were subjected to HPLC fractionation, and mass (MH^+) of peptides was determined by MALDI-TOF MS. The peptides containing the proposed DAPK phosphorylation sites in CaMKKβ (peptide 1) and syntaxin 1A (peptide 5) were the only ones that increased in mass by +80 MH^+, consistent with a monophosphorylated site. Peptides 2−4 and 6−7 are control peptides from CaMKKβ and syntaxin 1A that contain serine or threonine residues, including the CaMKKβ peptide that contains the PKA site (peptide 2). These peptides did not increase in mass upon DAPK treatment.

As summarized in Table 1, the peptide containing the proposed DAPK phosphorylation site serine in CaMKK was found to undergo the expected shift in peptide mass. The extended sequence (...RREERSLSAPGNLLTK...) containing the potential DAPK phosphorylation site is cleaved by trypsin into several peptides. One of these peptides has a computed mass of 1100.26 MH^+ and contains the phosphorylation site serine, as well as additional serine and threonine residues (SLSAPGNLLTK). Stoichiometric phosphorylation of CaMKK by DAPK would theoretically yield a peptide with a computed mass of 1180.26 MH^+ (Table 1, peptide 1). Experimentally, we found a peptide of mass 1180.10 (Table 1, peptide 1). Other peptides containing serine or threonine residues but lacking the preferred DAPK motif in their sequences were also recovered and analyzed as controls. Their experimentally determined mass matched well their unphosphorylated computed masses whether they were isolated from digests of the DAPK-phosphorylated CaMKK or the unphosphorylated CaMKK control. These peptides included peptide 2 (SFGNPFEGSR), which contains a serine

Table 2: Confirmation by Site-Directed Mutatgenesis of DAPK Phosphorylation Site in CaMKK and Comparison of DAPK Substrate Proteins[a]

Protein	K_m	Phosphorylation Site Sequence
CaMKKβ (K194A)	3 μM	...RREERSL**S**APGNLLTK...
CaMKKβ (K194A, S511A)	-	...RREERSL**A**APGNLLTK...
CaMKKβ (K194A, S509A)	8 μM	...RREER**A**LSAPGNLLTK...
CaMKKβ (K194A, T518A)	3 μM	...RREERSLSAPGNLL**A**K...
Syntaxin 1A	5 μM	...IIMDSSI**S**KQALSEIE...
MLC	65 μM	...KRPQRAT**S**NVFAMFDQ...

[a] All CaMKKβ substrates contain the K194A substitution to prevent autophosphorylation. CaMKKβ(K194A,S511A) has the proposed phosphorylated serine removed by the S511A mutation; this protein did not incorporate sufficient phosphate to allow a K_m determination. In contrast, mutation of the nearby Ser509 or Thr518 side chains to alanine did not significantly affect the estimated K_m values. The potential phosphorylated residue or its corresponding alanine mutation in the phosphorylation site of each sequence is bold.

that is phosphorylated by PKA (*17*). To confirm the apparent divergent site utilization in protein substrates linked to two distinct signaling pathways and physiological end points, we extended the analysis to syntaxin 1A. Peptide 5 (Table 1) from syntaxin 1A undergoes a shift of +80 MH^+ as a result of DAPK phosphorylation of syntaxin 1A, demonstrating that it contains the phosphorylated serine. Alignment with the syntaxin 1A ORF confirms the phosphorylation site identified previously (*15*) by site-directed mutagenesis.

The mapping of the DAPK phosphorylation site in CaMKK by MALDI-TOF MS identified the peptide and the relative location of the phosphorylation site within CaMKK, showing that it is distinct from that phosphorylated by PKA. Although serine 511 (S511) is the predicted phosphate-acceptor amino acid in peptide 1 (Table 1) based on the prior (*5*) docking and scanning synthetic peptide substrate analyses, there are two serines and a threonine in the peptide 1 sequence (SLSAPGNLLTK). Confirmation of the predicted residue was done experimentally by site-directed mutagenesis of the serine to an alanine and testing of the mutant protein for its ability to serve as a DAPK substrate. The S511A mutation in CaMKK resulted in a severe loss in DAPK phosphorylation (Table 2). In contrast, control mutations (S509A or T518A) within this same region of CaMKK did not result in significant changes in the estimated K_m values. Phosphorylation of CaMKK by DAPK at S511 was further demonstrated by Western blot analysis (Figure 3A) of GST−CaMKKβ(K194A) phosphorylated in vitro by DAPK. The site-directed antisera were made by use of a peptide antigen phosphorylated at the serine residue corresponding to S511 in CaMKKβ. As shown in Figure 3A, phosphorylated CaMKK is detected by the antisera, but unphosphorylated CaMKK and DAPK alone are not detected. As anticipated by its kinetic and substrate recognition properties, DAPK is able to catalyze this site-specific phosphorylation of endogenous CaMKK in the context of a living cell. As shown in Figure 3B, there is an increase in phosphorylation of endogenous human CaMKK at S511 when SH-SY5Y cells are transfected with a plasmid encoding constitutively active human DAPK. CaMKK protein levels by Western blot do not change (data not shown). Overall, the data identify S511 in CaMKKβ as the DAPK phosphorylated amino acid and show that the site preferred by DAPK in CaMKK has a distinct amino acid motif from that recognized by DAPK in syntaxin 1A.

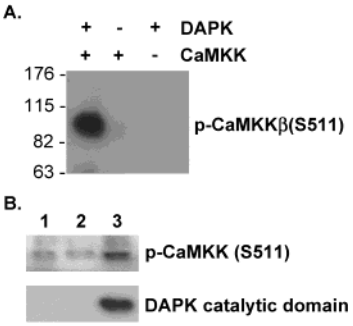

FIGURE 3: Western blot detection of CaMKK phosphorylation at S511 by DAPK in vitro and in cells. In panel A, phosphorylation of GST−CaMKKβ(K194A) by DAPK was done in vitro as described in Experimental Procedures. Equal amounts of each reaction were resolved by SDS−PAGE and visualized by Western blotting with a site-directed CaMKK antisera directed against phosphorylated S511. The phosphorylated form of the M_r = 92 000 fusion protein, GST−CaMKKβ(K194A), is detected. In panel B, overexpression of DAPK increases phosphorylation of endogenous CaMKKβ at S511 in cells as determined by Western blotting. SH-SY5Y cells were either untransfected (lane 1), transfected with GFP control plasmid (lane 2), or transfected with DAPK (lane 3). Cells were collected 6 h after transfection and equal amounts of protein were used for Western blotting. Note that increased phosphorylation of CaMKK is detected upon expression of the constitutively active DAPK catalytic domain protein. Data shown are representative of two independent experiments.

Effect of DAPK Phosphorylation of CaMKK on CaM-Induced Autophosphorylation. The location of the DAPK phosphorylation site in CaMKK at S511, adjacent to the CaM recognition segment (Figure 4A), raises the possibility that CaM activation of CaMKK may be altered upon phosphorylation by DAPK. This would be similar to the prior finding (*17*) that PKA phosphorylation of CaMKKα at S458 (equivalent to S495 in CaMKKβ) interferes with CaM regulation of CaMKK. Therefore, we examined the effects of DAPK phosphorylation of CaMKK at S511 on CaM activation of CaMKK autophosphorylation. As shown in Figure 4B, CaM-dependent autophosphorylation of CaMKK was attenuated by prior phosphorylation of CaMKK by DAPK. Note that the left lane shows background CaMKK autophosphorylation and that addition of Ca^{2+}/CaM stimulates autophosphorylation (Figure 4B, second lane). Under the conditions used here, there was an approximately 40% reduction in CaMKK autophosphorylation after DAPK phosphorylation, as determined by densitometry analysis of the phosphor-image. To confirm that the effect of DAPK on CaMKK autophosphorylation was due to phosphorylation of S511 in CaMKKβ, we examined CaM-dependent autophosphorylation of CaMKK with an S511A substitution in the presence of DAPK. As shown in Figure 4C, DAPK did not suppress CaM-induced CaMKK autophosphorylation when S511 was changed to an unphosphorylatable residue.

DISCUSSION

There are six key aspects of the research presented here. First, we identified CaMKK as the first substrate of DAPK

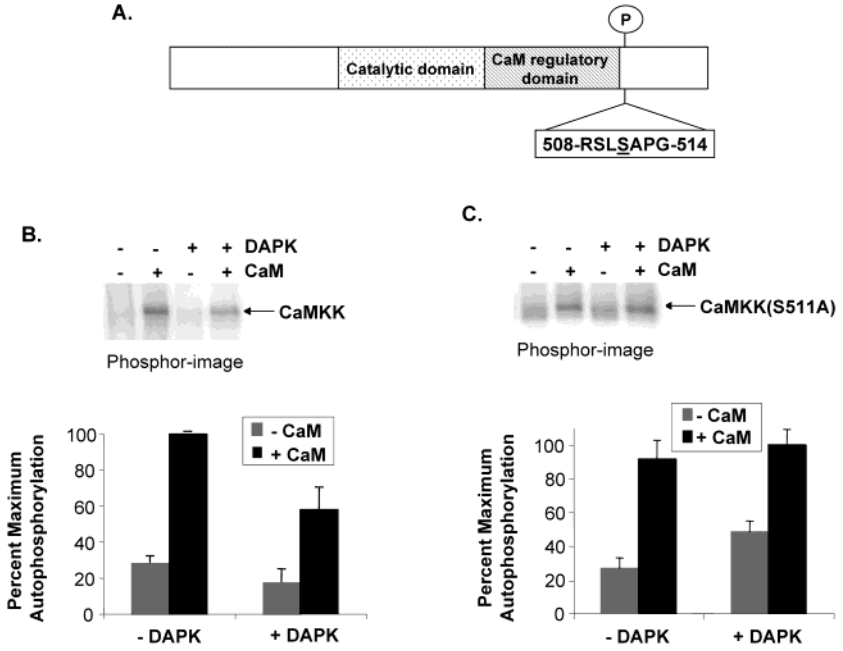

FIGURE 4: Suppression of CaM-stimulated CaMKK autophosphorylation by DAPK phosphorylation of CaMKK. In panel A, the schematic indicates the relative location of the DAPK phosphorylation site within the CaMKK amino acid sequence, adjacent to the CaM regulation domain. In panel B, the effects of DAPK phosphorylation of CaMKK on CaM-dependent CaMKK autophosphorylation are shown. CaM stimulation of CaMKK autophosphorylation was assayed after phosphorylation by DAPK. CaMKK was first phosphorylated by DAPK in the presence of nonradioactive ATP; then autophosphorylation was monitored by addition of [γ-^{32}P]-ATP to the reaction mix, subjection of samples to SDS−PAGE, and detection by phosphor-imaging of gels. Densitometry analysis of the CaMKK band was done to quantify the extent of autophosphorylation. CaM-activated autophosphorylation in the absence of DAPK is taken to be 100%. The phosphor-image shown is representative of three independent experiments, and densitometry results are the average of three experiments. Error bars represent mean ± SEM. Panel C shows the effects of DAPK on CaM-dependent autophosphorylation of a mutant CaMKK with the phosphorylatable serine (S511) changed to alanine. Analysis was done as described for panel B. Phosphor-image shown is representative of three experiments, and densitometry results are the average of three experiments. Error bars represent mean ± SEM.

relevant to the role of DAPK in brain injury and to DAPK as a drug-discovery target in neurodegeneration. Second, we mapped the DAPK phosphorylation site in CaMKK to S511, found in a sequence adjacent to the CaM recognition domain. Third, consistent with the location of S511 within CaMKK, we showed that DAPK phosphorylation has a negative effect on CaM-induced CaMKK autophosphorylation. Because CaMKK was previously shown (*14*) to be key for neuronal survival, DAPK-mediated inhibition of CaMKK could potentially bring about apoptosis by a decrease in neuronal survival pathways. Fourth, we showed that DAPK phosphorylates CaMKK at a single site and with a K_m value that falls within the definitive range of physiological substrates for protein kinases functioning as components of intracellular signaling cascades. Consistent with these features, we showed that DAPK phosphorylates endogenous CaMKK at this site in human cells. Fifth, we showed by comparative peptide mapping using mass spectrometry and by comparative kinetic analyses of brain syntaxin 1A and CaMKK that two distinct phosphorylation site sequences are used by DAPK in these neuronal proteins linked to divergent physiological pathways. Sixth, we validate a generalizable approach to the identification of endogenous protein substrates for kinases identified in the absence of knowledge about biochemical context. The results presented here, therefore, identify new potential molecular mechanisms for DAPK-mediated regulation of intracellular phosphorylation pathways, bring a convergence between previously unconnected areas of research, and provide insight that may facilitate the further development of new therapeutic approaches to neurodegenerative diseases.

The plausible link of DAPK to neuronal apoptosis via phosphorylation of another CaM-regulated protein kinase is based on the interpretation of our results in the context of previous reports on CaMKK as a regulatory component of a neuronal survival signaling pathway. For example, CaMKK phosphorylation of Akt was shown (*14*) to be important in the protection of neurons from apoptosis. In addition, CaMKK phosphorylates other CaM-regulated protein kinases (*18*) such as CaMKIV, which has been implicated in activation of MAPK cascades and subsequent inhibition of apoptosis (*19*). Therefore, attenuation of CaMKK-mediated pathways due to an upstream event such as phosphorylation by DAPK might provoke cell death through the loss of more than one survival pathway. Clearly, much remains to be done in terms of how DAPK phosphorylation of CaMKK is related to downstream pathophysiology and responses to therapy, but the results reported here provide a focus and firm foundation for such future biological investigations and raise the possibility of CaM kinase-mediated signal transduction pathways as being integral components.

Suppression of CaM-dependent CaMKK autophosphorylation by DAPK is reflective of a redundant theme in CaM-regulated signal transduction pathways. The location of the DAPK phosphorylation site in CaMKK is adjacent to the CaM recognition domain of CaMKK. The theme of signal transduction cross-talk involving regions adjacent to the CaM recognition domain was first established with the extensively characterized DAPK-like protein MLCK (*12*, *20*) and extended more recently to CaMKK (*17*). However, the novel variation of the theme employed with CaMKK and DAPK

in apoptosis is that two calcium- and CaM-regulated enzymes are involved in an apparent cascade versus cross-talk between two different second-messenger-mediated pathways.

Our results are the first direct comparisons of protein substrates for DAPK and the first demonstration that divergent phosphorylation site sequences are present in protein substrates with similar kinetic properties. The approximate K_m values of CaMKK and syntaxin 1A for DAPK reported here are within the range of values (1−20 μM) characteristic of physiological substrates for signal-transducing protein kinases, consistent with diverse protein substrate phosphorylation site sequences being associated with potentially discrete biological functions. Further, the novel activity and protein chemistry results reported here are consistent with our previous homology modeling and peptide substrate library analyses that provided initial insight into the strict substrate requirements of DAPK compared to most CaM kinases but more relaxed compared to the most stringent of all CaM kinases, MLCK (*21*). The previous results from homology modeling of the DAPK crystal structure with a peptide substrate revealed (*5*) that diverse amino acid sequences immediately adjacent to the phosphorylatable residue could be accommodated but only serine or threonine (and not tyrosine) was allowable as the acceptor amino acid. Results (*5*) with synthetic peptides confirmed the docking model. The amino acids present in the peptide substrates outside of but proximal to the core phosphorylation sequence were also shown (*5*) to be major contributors to peptide substrate utilization by DAPK. This suggested that the overall context of the phosphorylation site within a potential protein substrate could be equally important. The results reported here comparing CaMKK and syntaxin 1A as substrates are consistent with this prevailing hypothesis.

Overall, the results presented here and previously (*2*, *5*) add to the validation of the structure-assisted, de novo approach to inhibitor and substrate discovery for protein kinases, as well as filling a void in knowledge and providing insight into potential regulatory pathways. The extension of the informatics based results to future investigations may be especially useful. For example, refinement of the phosphosite pattern in the upstream and downstream directions based on sequence information garnered from the quantitative protein substrate data (CaMKK, syntaxin 1A, and MLC) can be used to reiteratively explore sequence databases with ScanProsite (http://us.expasy.org/tools/scanprosite). These searches reveal only a couple hundred hits, many of which are isoforms of the known substrates. The remaining hits can be grouped into functional categories, revealing approximately 50 hits related to apoptosis, tumor suppression, and synaptic trafficking—all potentially relevant to DAPK signal-transduction pathways. The recursive refinement of the knowledge base of DAPK substrates, both peptide and protein, suggests logical groups of proteins to be investigated as candidates for DAPK protein substrates in future research. Clearly, much remains to be done, and ongoing biological investigations are a required extension of the findings reported here. However, the generalizable approach combined with targeted reagents (e.g., anti-phosphosite antibodies) should provide a firmer foundation for in vivo chemical biology studies using bioavailable small molecule inhibitors (*2*) by allowing a closer linkage of endogenous protein phosphorylations to biological end points.

ACKNOWLEDGMENT

A.M.S. is a predoctoral scholar and A.V.V. was a postdoctoral scholar in the Drug Discovery Training Program.

REFERENCES

1. Schumacher, A. M., Velentza, A. V., and Watterson, D. M. (2002) Death associated protein kinase as a potential therapeutic target, *Expert Opin. Ther. Targets 6*, 497−506.
2. Velentza, A. V., Wainwright, M. S., Zasadzki, M., Mirzoeva, S., Schumacher, A. M., Haiech, J., Focia, P. J., Egli, M., and Watterson, M. (2003) An aminopyridazine based inhibitor of a pro-apoptotic protein kinase attenuates hypoxia-ischemia induced acute brain injury, *Bioorg. Med. Chem. Lett. 13*, 3465−3470.
3. Krebs, E. G., and Fischer, E. H. (1956) The phosphorylase b to a converting enzyme of rabbit skeletal muscle, *Biochim. Biophys. Acta 20*, 150−157.
4. Kopperud, R., Krakstad, C., Selheim, F., and Doskeland, S. O. (2003) cAMP effector mechanisms. Novel twists for an 'old' signaling system, *FEBS Lett. 546*, 121−126.
5. Velentza, A. V., Schumacher, A. M., Weiss, C., M., Egli, M., and Watterson, D. M. (2001) A protein kinase associated with apoptosis and tumor suppression: Structure, activity, and discovery of peptide substrates, *J. Biol. Chem. 276*, 38956−38965.
6. Krebs, E. G., and Rosen, O. M. (1981) Summary, in *Protein Phosphorylation* (Rosen, O. M., and Krebs, E. G., Eds.) pp 1407−1412, Cold Spring Harbor Laboratories, New York.
7. Schumacher, A. M., Velentza, A. V., Watterson, D. M., and Wainwright, M. S. (2002) DAPK catalytic activity in the hippocampus increases during the recovery phase in an animal model of brain hypoxic-ischemic injury, *Biochim. Biophys. Acta 1600*, 128−137.
8. Edelman, A. M., Blumenthal, D. K., and Krebs, E. G. (1987) Protein serine/threonine kinases, *Annu. Rev. Biochem. 56*, 567−613.
9. Watterson, D. M., Collinge, M., Lukas, T. J., Van Eldik, L. J., Birkukov, K. G., Stepanova, O. V., and Shirinsky, V. P. (1995) Multiple gene products are produced from a novel protein kinase transcription region, *FEBS Lett. 373*, 217−220.
10. Fabre, S., Prudhomme, M., and Rapp, M. (1993) Protein kinase C inhibitors; structure−activity relationships in K252c-related compounds, *Bioorg. Med. Chem. 1*, 193−196.
11. Watterson, D. M., and Vanaman, T. C. (1976) Affinity chromatography purification of a cyclic nucleotide phosphodiesterase using immobilized modulator protein, a troponin C-like protein from brain, *Biochem. Biophys. Res. Comm. 73*, 40−46.
12. Lukas, T. J., Burgess, W. H., Prendergast, F. G., Lau, W., and Watterson, D. M. (1986) Calmodulin binding domains: characterization of a phosphorylation and calmodulin binding site from myosin light chain kinase, *Biochemistry 25*, 1458−1464.
13. Van Eldik, L. J., Fok, K. F., Erickson, B. W., and Watterson, D. M. (1983) Engineering of site-directed antisera against vertebrate calmodulin by using synthetic peptide immunogens containing an immunoreactive site, *Proc. Natl. Acad. Sci. U.S.A. 80*, 6775−6779.
14. Yano, S., Tokumitsu, H., and Soderling, T. R. (1998) Calcium promotes cell survival through CaM-K kinase activation of the protein-kinase-B pathway, *Nature 396*, 584−587.
15. Tian, J.-H., Das, S., and Sheng, Z.-H. (2003) Ca^{2+}-dependent phosphorylation of syntaxin-1A by DAP-kinase regulates its interaction with munc-18, *J. Biol. Chem. 278*, 26265−26274.
16. Cohen, O., Feinstein, E., and Kimchi, A. (1997) DAP-kinase is a Ca^{2+}/calmodulin-dependent, cytoskeletal-associated protein kinase, with cell death-inducing functions that depend on its catalytic activity, *EMBO J. 16*, 998−1008.
17. Wayman, G. A., Tokumitsu, H., and Soderling, T. R. (1997) Inhibitory cross-talk by cAMP kinase on the calmodulin-dependent protein kinase cascade, *J. Biol. Chem. 272*, 16073−16076.
18. Tokumitsu, H., Enslen, H., and Soderling, T. R. (1995) Characterization of a CaM-kinase cascade: molecular cloning and characterization of CaM-kinase, *J. Biol. Chem. 270*, 19320−19324.

19. Enslen, H., Tokumitsu, H., Stork, P. J., Davis, R. J., and Soderling, T. R. (1996) Regulation of MAP kinases by a calcium/calmodulin-dependent protein kinase cascade, *Proc. Natl. Acad. Sci. U.S.A.* 93, 10803−10808.
20. Shoemaker, M. O., Lau, W., Shattuck, R. L., Kwiatkowski, A. P., Matrisian, P. E., Guerra-Santos, L., Wilson, E., Lukas, T. J., Van Eldik, L. J., and Watterson, D. M. (1990) Use of DNA sequence and mutant analyses and antisense oligodeoxynucleotides to examine the molecular basis of nonmuscle myosin light chain kinase autoinhibition, calmodulin recognition, and activity, *J. Cell Biol. 111*, 1107−1125.
21. Lukas, T. J., Mirzoeva, S., and Watterson, D. M. (1998) Calmodulin-regulated protein kinases, in *Calmodulin and Signal Transduction* (Van Eldik, L., and Watterson, D. M., Eds.) pp 65−168, Academic Press, New York.

BI049589V